HIGH FIELD MRS OF NEUROTRANSMITTERS

PETER S ALLEN, CHANGHO CHOI AND CHRIS C HANSTOCK

DEPT OF BIOMEDICAL ENGINEERING, UNIVERSITY OF ALBERTA, CANADA

INTRODUCTION

What are the neurotransmitters that an NMR system might be able to see?: Three major categories of substances can act as neurotransmitters, namely, amino acids, monoamines and peptides, but only the amino acid neurotransmitters, e.g., glutamate [Glu], γ-aminobutyric acid [GABA], aspartate [Asp] and glycine [Gly], reside with sufficient concentration in brain to be detected in-vivo with today's one-metre-bore NMR hardware. In spite of this limitation, the amino acid neurotransmitters can provide a wealth of information about normal and compromised brain function because their metabolism is key to those functions (1).

Why are the amino acid neurotransmitters so influential in controlling brain function?: A satisfactory answer to this question is clearly beyond the scope of this talk. Nonetheless, the significant role that NMR has played in the clarification of how the major workhorse transmitters, Glu (along with its sidekick glutamine [Gln]) and GABA function within the tightly coupled neuron-astrocyte system in normal brain, can be seen from the work of several groups. References (2-5) are just a small selection from these.

What do the amino acid neurotransmitters look like if you are an r.f. coil, surrounding a head, lying inside a magnetic field?: Within the published literature it is usual to find the proton used for the measurement of steady-state neurotransmitter concentrations, whereas dynamic measurements of metabolite fluxes usually exploit the ^{13}C nucleus. We shall indicate schematically in Figs (1) to (4) how the neurotransmitter molecular structure affects first, the proton spectrum and secondly, the ^{13}C NMR spectrum in Glu, Gln and GABA. These diagrams illustrate the nuclear coupling schemes (6, 7) and their rudimentary 90º-acquire spectra at the not-so-high field strength of 3.0 T, thus reflecting a worst-case scenario for spectral resolution at the lowest level of the "high field" range. It must also be borne in mind that the molecular structure is important to the understanding of the dynamic changes that occur in the NMR spectra during the measurement of the chemical rate processes that take place during metabolism (8).

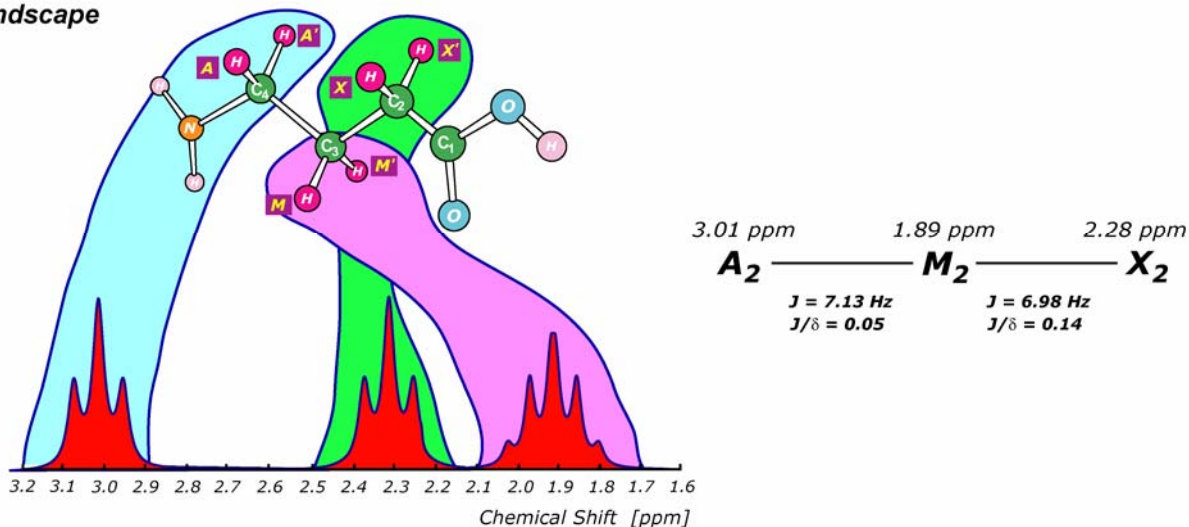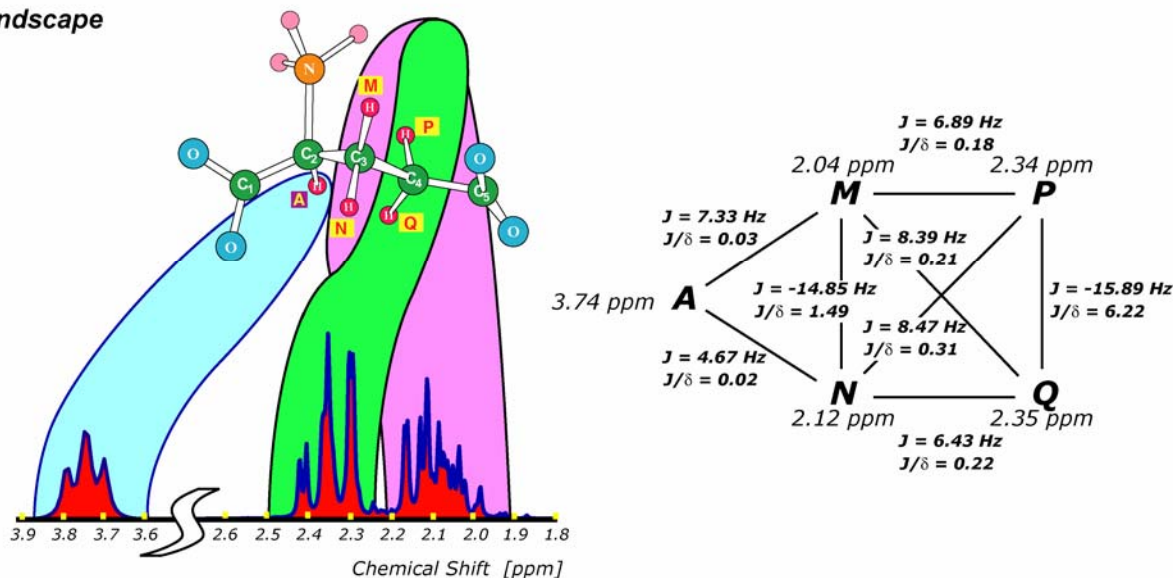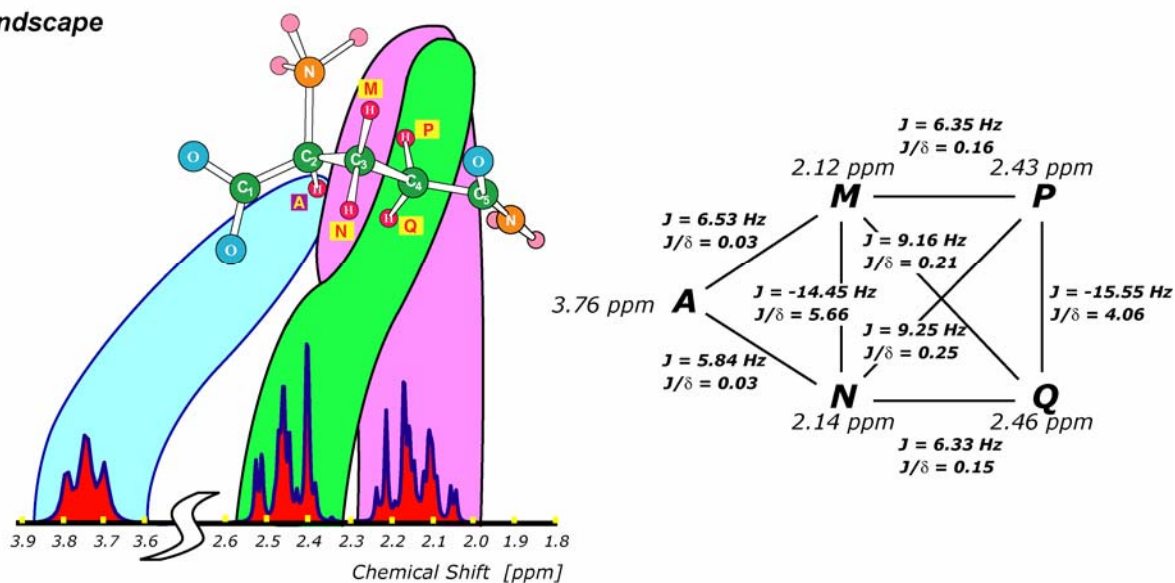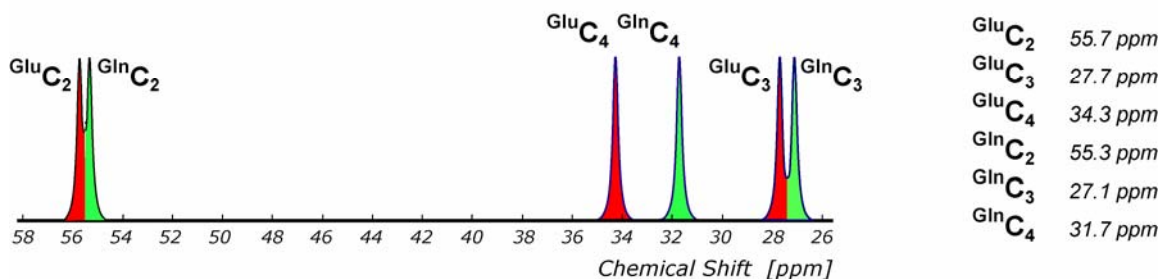## Fig 1   GABA: Its Vital Signs and its Spectrum at 3.0 T

Fig 2   Glutamate: Its Vital Signs and its Spectrum at 3.0 T

Proton Landscape

$J = 6.89$ Hz
$J/\delta = 0.18$
2.04 ppm   2.34 ppm
M ————————— **P**

$J = 7.33$ Hz
$J/\delta = 0.03$

$J = 8.39$ Hz
$J/\delta = 0.21$

3.74 ppm **A** $J = -14.85$ Hz $J = -15.89$ Hz
$J/\delta = 1.49$ $J/\delta = 6.22$

$J = 8.47$ Hz
$J/\delta = 0.31$

$J = 4.67$ Hz
$J/\delta = 0.02$

N   **Q**
2.12 ppm   2.35 ppm
$J = 6.43$ Hz
$J/\delta = 0.22$

Chemical Shift [ppm]
3.9 3.8 3.7 3.6   2.6 2.5 2.4 2.3 2.2 2.1 2.0 1.9 1.8

Fig 3   Glutamine: Its Vital Signs and its Spectrum at 3.0 T

Proton Landscape

$J = 6.35$ Hz
$J/\delta = 0.16$
2.12 ppm   2.43 ppm
M ————————— **P**

$J = 6.53$ Hz
$J/\delta = 0.03$

$J = 9.16$ Hz
$J/\delta = 0.21$

3.76 ppm **A** $J = -14.45$ Hz $J = -15.55$ Hz
$J/\delta = 5.66$ $J/\delta = 4.06$

$J = 9.25$ Hz
$J/\delta = 0.25$

$J = 5.84$ Hz
$J/\delta = 0.03$

N   **Q**
2.14 ppm   2.46 ppm
$J = 6.33$ Hz
$J/\delta = 0.15$

Chemical Shift [ppm]
3.9 3.8 3.7 3.6   2.6 2.5 2.4 2.3 2.2 2.1 2.0 1.9 1.8

Fig 4   Glu & Gln: Vital Signs and Spectrum at 3.0 T

Proton-Decoupled Carbon Landscape

$^{Glu}C_4$ $^{Gln}C_4$

$^{Glu}C_2$ $^{Gln}C_2$ $^{Glu}C_3$ $^{Gln}C_3$

58 56 54 52 50 48 46 44 42 40 38 36 34 32 30 28 26
Chemical Shift [ppm]

$^{Glu}C_2$ 55.7 ppm
$^{Glu}C_3$ 27.7 ppm
$^{Glu}C_4$ 34.3 ppm
$^{Gln}C_2$ 55.3 ppm
$^{Gln}C_3$ 27.1 ppm
$^{Gln}C_4$ 31.7 ppm

What measurement problems are ameliorated by an increase in the magnetic field strength: The greatest NMR induced hindrance to accuracy and precision in neurotransmitter proton spectroscopy is

the small chemical-shift range of the proton. Not only does it lead to substantial spectral overlap, but for Glu, Gln and Asp it also leads to strong inter-proton scalar coupling effects. The inter-proton polarization transfer that occurs due to this strong coupling modulates both the amplitude and the lineshape of a strongly-coupled proton spectrum in a manner different from that of weakly-coupled spin systems, and it is dependent on both pulse intervals and the pulses themselves. As a result a target neurotransmitter spectrum in relation to its contaminating background spectra will be quite dependent on the details of the localizing sequence design. Higher fields increase the chemical-shift dispersion and thereby reduce the relative strength of the scalar coupling. This not only ameliorates some of these dependencies, but also gives rise to more spin-manipulation "elbow room" that makes editing easier.

The biggest problem for *direct* ^{13}C spectroscopy is its low signal to noise ratio (SNR), arising from a combination of low gyromagnetic ratio and low natural abundance. The latter however, is the key to its power to provide the dynamic measurements of time-dependent ^{13}C enrichments at specific molecular sites, that in turn reflect metabolic flux rates. Higher fields increase SNR so that reduced averaging enables the temporal resolution of the time-dependent enrichments to be increased for a given SNR. The strong inter-proton scalar coupling affects both the *direct* observation of the ^{13}C spectrum (by changing hetero-nuclear polarization transfer enhancements) and the *indirect* detection of ^{13}C using surrogate proton signals (by inducing cross-talk between the proton multiplets) (9). The increase in proton chemical-shift dispersion with increasing field strength, relative to the proton scalar coupling, reduces both of these effects.
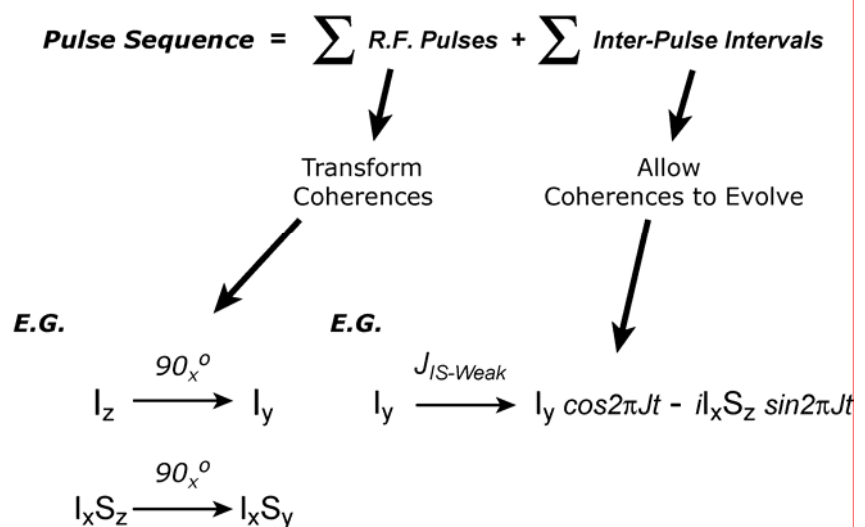
The following section and the multitude of citations are meant to provide a wide reference bas from which the key points will be discussed in the talk.

THE SINGLE VOXEL METHODS COMMONLY APPLIED TO AMINO ACID NEUROTRANSMITTERS

Scope: Even discussing all the single-voxel methods in detail is beyond the scope of a short talk, I shall therefore concentrate on the physical underpinnings, with references to specific methods that best seem able to take advantage of these underpinnings for evaluating the amino acid neurotransmitters using protons or ^{13}C. High quality shimming will be assumed throughout. A fairly recent review of ^{13}C spectroscopy (10) includes a significant discussion of the ^{13}C methodology.

Sequence Generalities: All localizing MRS sequences contain r.f. pulses, gradient pulses and the pulse intervals between them. As experimenters we would hope to find that the only effects of these sequence components were the effects for which they were designed, e.g., production and refocussing of transverse magnetization, localization of signal acquisition, phase encoding of spatial or spectral parameters, etc.. However, the interactions between spins often cause other things to happen in parallel, e.g., the effect of transverse relaxation

Fig. 5 What Happens in a Spectroscopy Experiment ?

$$\text{Pulse Sequence} = \sum \text{R.F. Pulses} + \sum \text{Inter-Pulse Intervals}$$

Transform Coherences   Allow Coherences to Evolve

E.G.   E.G.

$$I_z \xrightarrow{90_x^o} I_y \qquad I_y \xrightarrow{J_{IS\text{-}Weak}} I_y \cos 2\pi Jt - iI_x S_z \sin 2\pi Jt$$

$$I_x S_z \xrightarrow{90_x^o} I_x S_y$$

is well known. The effects of scalar coupling are a bit more complex (see Fig (5)), and while some are a handicap, others are a boon. In general terms, and bearing in mind that many of the key brain

metabolites (not only some neurotransmitters) contain spins that are strongly coupled, a significant consequence of scalar coupling is that signal-generating transverse magnetization is spectrally dispersed and often lost in the creation and evolution of unobservable coherences. This means that the signal intensity is typically less than one might expect (reduced yield) by assuming transverse relaxation to be the only signal loss mechanism. The unobservable coherences can arise between the r.f. pulses through scalar-coupled evolution, and during the r.f. pulses through evolutions and through various experimental imperfections. As a result, the spectral response of a brain metabolite to a localizing pulse sequence is usually quite different from what it would be to a single-pulse-acquire sequence. In brain this is typically true for both a target metabolite and for the metabolites that give rise to the contaminating background. However, even though anti-phase and multiple quantum coherences can't be seen, they can still be manipulated, and by appropriate design of sequences, particularly editing sequences but also to some extent PRESS or STEAM (11), background contamination can be reduced (thereby making outcome of post-processing strategies such as LCModel (12) more reliable), or even eliminated. A decade ago the design of multiple quantum filters enabled them to separate coupled-spin species (both weakly and strongly coupled species jointly) from uncoupled species. However, more recent developments (13,14) have shown that they can also be designed to separate strongly coupled species from both weakly coupled and uncoupled species jointly.

GABA: For GABA, the low concentration taken together with the particular chemical shifts of each of its three proton multiplets, makes background contamination the most serious problem to its quantification by proton spectroscopy. In consequence, some form of editing is almost always used. GABA lends itself well to editing because at 3.0 T and above, its spin system satisfies the weak-coupling limit. This is hardly true at 1.5 T (15). The GABA A_2 multiplet at 3.01 ppm, having a contaminating background from creatine (t-Cr-PCr), glutathione (GSH), homocarnosine, and macromolecules, is the most popular GABA target, although the X_2 multiplet (with a different background) has been exploited (11) to quantify GABA in the human brain. The homocarnosine, GSH and the macromolecular background resonances near 3.0 ppm, all have scalar-coupling partners. Those of homocarnosine are closest to those of GABA. The original editing method for GABA, (whose evolutionary derivative is still in use after more than a decade) was a difference methodology pioneered by the Yale group (16,17). To avoid difference editing, a richness of other techniques has been proposed (18-22) that finds alternative ways to separate a GABA multiplet from its background. These include a number of multiple quantum filters, some of which (18-21) exploit doubly-frequency-selective pulses in order to manipulate the A_2 and the M_2 spins of GABA selectively and concurrently, and make the editing more specific to GABA than to its coupled-spin background. Another important feature (19) reintroduces some original r.f. pulse design work of Geen and Freeman (23), (used elsewhere in a Glu filter (24) to eliminate the chemical shift dispersion in the initial transverse magnetization) to control the spin dynamics during a pulse whose role is concurrently spatial selectivity and coherence transfer. Efforts to quantify GABA also include a novel proposition (25), verified on rats at 11.4 T, to clear all signals from the 3.0 ppm spectral region at the beginning of the sequence, and then regenerate a GABA A_2 multiplet by polarization transfer from the M_2 spins. There are strategic similarities between this proposition and a localized TOCSY technique (26) for recovering weak signals from a totally suppressed part of the spectrum. An alternative to 1D spectral editing is to allow the spin evolution to play out in time while acquiring the transverse magnetization decay signal at successively incremented play-out time points. A data set in two time dimensions is therefore produced which permits a representation of the spectrum as a two-dimensional map with different spectral parameters e.g., scalar coupling strength, *J,* and chemical shift, δ, along the two axes of the map. Although a number of groups have explored this strategy at 3.0 T and 4.0 T respectively (27,28), the success which these groups have had with GABA does not appear to have surpassed that achieved with 1D editing.

Glu - Gln: The separation and quantification of Glu and Gln from the proton spectrum of brain is quite different from that of separating GABA from its background. This is because the key protons of Glu and Gln are strongly coupled. To reach the weak-coupling limit for all their couplings will require $B_o >$ 100 T, however the PQ to MN couplings will be in their weak limit by $\sim$ 18 T. What is more, their molecular structures are so similar that, as shown in Figs 2 and 3, their proton chemical shifts and coupling schemes are really difficult to distinguish. Although multiple quantum filters have been published (24), recourse is typically taken, first, in moving to higher field strengths, and secondly, following a variant of a standard localization sequence, e.g., STEAM (29-33) or PRESS (34-37), in the LCModel. The Minnesota group has been particularly successful with short-echo STEAM on rats at 9.4 T (29,30), shortening the {TE, TM} time coordinates of STEAM to {$\leq$ 2 ms, $\leq$ 20 ms} in order to beat the polarization transfer, which arises from strong coupling and which spoils the evolutionary *J*-modulation that is easier to handle. A similar strategy has been employed at 7.0 T on monkeys (31) with time coordinates {TE, TM} = {10 ms, 10 ms}. Figure 6 illustrates the variation of the peak height of the central peak of the PQ multiplet of Glu as a function of these time coordinates of the STEAM sequence at different field strengths. It emphasises not only the non-monotonic dependence of Glu signal intensity on those times and the rapid decay with TE, but it also demonstrates particularly, the exacerbation of the periodic dependence on TM as the field strength increases. The periodicity arises from the oscillations of the real and imaginary parts of the zero quantum coherence during TM, oscillations whose frequency depends on the chemical shift separation of the coupled spin species and hence the field dependence. A positive aspect of these periodic zeros in the Glx signal, is that they can be exploited for removing contaminating background due to Glx, from GABA X_2 signals for instance (11).

Fig. 6 Response of Central Peak Height of Glu PQ Multiplet to STEAM Timings
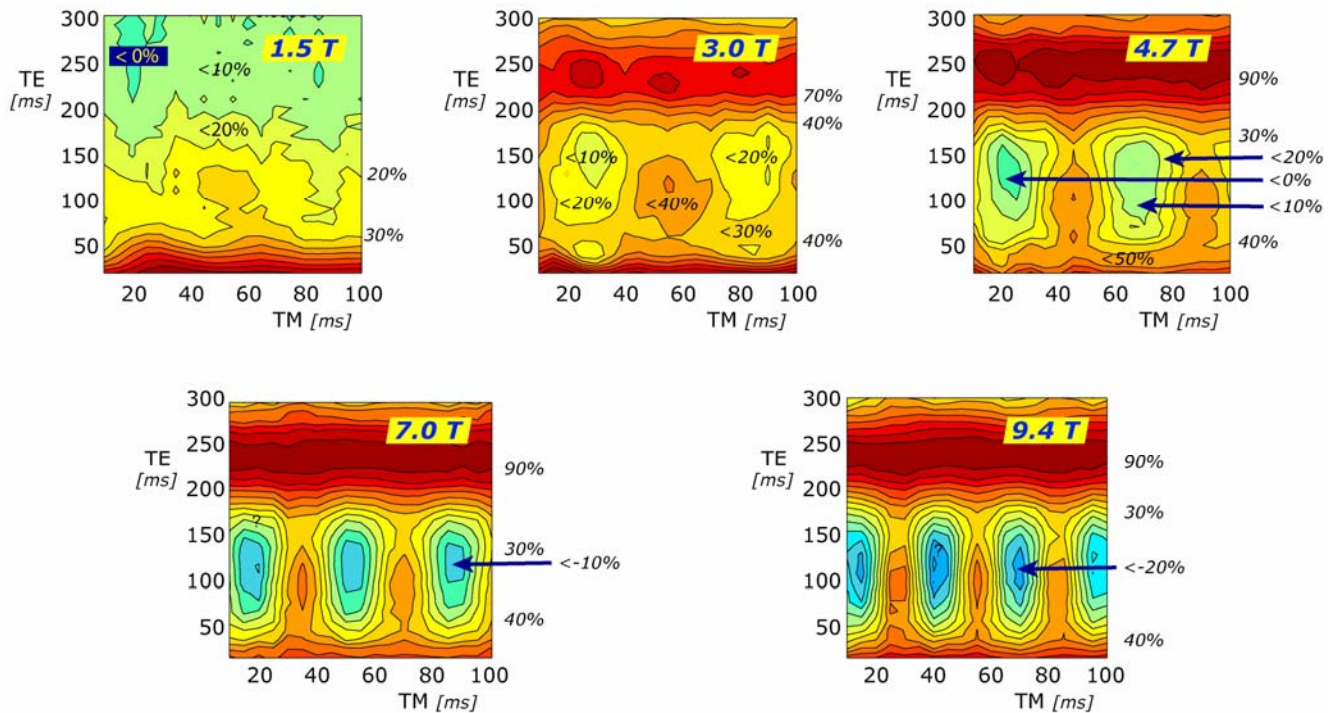
Proposals to mitigate the Glu strong-coupling effects in PRESS have included a short echo time sequence TE = 8 ms (34), an intermediate TE (80 ms) sequence (35), a longer effective-echo-time sequence (26 ms < TE_{eff} < 150 ms) that incorporates a non-slice-selective refocussing Carr-Purcell pulse train (36), and TE averaging (37). Representative Glu PQ multiplet intensity contours as a

function of the PRESS time coordinates {TE_1, TE_2} have been published (38), and while reflecting the underlying TE_1-v-TE_2 symmetry seen for weak coupling, they also demonstrate departures from it due to polarization transfer. The advantages of adiabatic pulses (39,40) in spin-echo localization have been thoroughly demonstrated by Kinchesh and Ordidge (41) using the LASER sequence (40).

The quantification of Glu and Gln by means of ^{13}C spectroscopy (10 and references therein) is linked to the proton spin system, either through the use of hetero-nuclear polarization transfer to enhance the ^{13}C SNR of the *direct* method of observation (42,43), or through the proton spectrum itself when *indirect* methods are used (44-46). However, the protons attached to the C_4 carbon position are strongly coupled to the protons attached to C_3, i.e., the PQ and MN protons respectively. This coupling has small but measurable effects on the hetero-nuclear polarization transfer of the *direct* method, but greater effects on the proton spectrum used in the *indirect* method (9). For example, as a result of this coupling the PQ multiplet is not independent of C_3 enrichment and neither is the MN multiplet independent of enrichments on C_4. Although an increasing field strength clearly enhances the SNR of both of these strategies, it is not likely to be great enough to change the strong inter-proton coupling situation. The *direct* detection method, with its much simpler interpretation, is therefore likely to benefit most from higher fields.

REFERENCES:

1. E.J. Novotny, R.K. Fulbright, P.L. Pearl, K.M. Gibson, D.L. Rothman. Magnetic Resonance Spectroscopy of Neurotransmitters in Human Brain. *Ann Neurol.* **54,** S25-S31 (2003).

2. P.J. Magistretti, L. Pellerin, D.L. Rothman, R.G. Shulman. Energy on Demand. *Science* **283,** 496-497 (1999).

3. J Shen, D.L. Rothman. Magnetic Resonance Spectroscopic Approaches to Studying Neuronal: Glial Interactions. *Biol Psychiatry* **52**, 694-700 (2002).

4. P. Morris, H Bachelard. Reflections on the Application of ^{13}C-MRS to Research on Brain Metabolism. *NMR Biomed* **16**, 303-312 (2003).

5. R.G. Shulman, D.L. Rothman, K.L. Behar, F. Hyder. Energetic basis of brain activity: implications for neuroimaging. *Trends Neurosci* **27,** 489-495 (2004).

6. V. Govindaraju, V.J. Basus, G.B. Matson, A.A. Maudsley. Measurement of Chemical Shifts and Coupling Constants for Glutamate and Glutamine. *Magn Reson Med* **39,** 1011-1013 (1998).

7. V. Govindaraju, K. Young, A.A. Maudsley. Proton NMR Chemical Shifts and Coupling Constants for Brain metabolites. *NMR Biomed* **13**, 129-153 (2000).

8. G.F. Mason, D.L. Rothman. Basic principles of metabolic modelling of NMR ^{13}C isotopic turnover to determine rates of brain metabolism in vivo. *Metab Eng* **6,** 75-84 (2004).

9. A. Yahya, P.S Allen. Effect of Strong Homonuclear Proton Coupling on Localized ^{13}C Detection Using PRESS. *Magn Reson Med* **54,** 1340-1350(2005).

10. R. Gruetter, G. Adriany, I-Y Choi, P-G Henry, H Lei, G Oz. Localized *in vivo* ^{13}C NMR spectroscopy of the brain. *NMR Biomed* **16**, 313-338 (2003).

11. C.C. Hanstock, N.J. Coupland, P.S. Allen. GABA X_2 Multiplet Measured Pre- and Post-Administration of Vigabatrin in Human Brain. *Magn Reson Med* **48,** 617-623 (2002).

12. S.W. Provencher. Estimation of metabolite concentrations from localized in vivo proton NMR spectra. *Magn Reson Med* **30,** 672-679 (1993).

13. A.H. Trabesinger, O.M. Weber, O.C. Duc, P. Bosiger, Detection of Glutothione in Human Brain by means of Double Quantum Coherence Filtering. *Magn Reson Med* **42,** 283-289 (1999).

14. H. Kim, J.M. Wild, P.S. Allen. Strategy for the Spectral Filtering of Myo-Inositol and Other Strongly Coupled Species. *Magn Reson Med* **51,** 263-272 (2004).

15. R.M. Thompson P.S. Allen Is GABA a Strongly-Coupled Spin System at 1.5 T? *Proc 8th Annual Meeting ISMRM (Denver)* p1859 (2000)

16. D.L. Rothman, O.A.C. Petroff, K.L Behar, R.H. Mattson. Localized ^{1}H NMR measurements of γ-aminobutyric acid in human brain *in vivo*. *Proc. Natl. Acad. Sci. USA* **90,** 5662-5666 (1993).

17. G.F Mason, I.L. Petrakis, R.A. de Graaf, R. Gueorguieva, E. Guidone, V. Coric, C.N, Epperson, D.L. Rothman, J.H. Krystal. Cortical Gamma-Aminobutyric Acid Levels and the Recovery from Ethanol Dependence: Preliminary Evidence of Modification by Cigarette Smoking. *Biol Psychiatry* **59,** 85-93 (2006).

18. J. Shen, D.L. Rothman, P. Brown. In vivo GABA Editing Using a Novel Doubly Selective Multiple Quantum Filter. *Magn Reson Med* **47,** 447-454 (2002).

19.   J. Shen. Slice-Selective *J*-Coupled Coherence Transfer Using Symmetric Linear Phase Pulses: Applications to Localized GABA spectroscopy. *J Magn Reson* **163,** 73-80 (2003).

20. I-Y. Choi, S-P. Lee, H. Merkle, J. Shen. Single-Shot Two-Echo Technique for Simultaneous Measurement of GABA and Creatine in the Human Brain In Vivo. *Magn Reson Med* **51,** 1115-1121 (2004).

21. C. Choi, N.J. Coupland, C.C. Hanstock, C.J. Ogilvie, A.C.M. Higgins, D. Gheorghiu, P.S. Allen. Brain γ-aminobutryic Acid Measurement by Proton Double-Quantum Filtering with Selective J Rewinding. *Magn Reson Med* **54** 272-279 (2005).

22. G. Bielicki, C. Chassain, J.P. Renou, M.C. Farges, M.P. Vasson, A. Eschalier, F. Durif. Brain GABA editing by localized *in vivo* ^{1}H magnetic resonance spectroscopy. *NMR Biomed* **17**, 60-68 (2004).

23. H. Geen, R. Freeman. Band-selective Radiofrequency Pulses. *J Magn Reson* **93,** 93-141 (1991).

24. R.B. Thompson, P.S. Allen. A New Multiple Quantum Filter Design Procedure for Use on Strongly-Coupled Spin Sytems Found In Vivo: Its Application to Glutamate. *Magn Reson Med* **39,** 762-771 (1998).

25. J Shen, J. Yang, I-Y. Choi, S.S. Li, Z. Chen. A New Strategy for In-Vivo Spectral Editing. Application to GABA Editing Using Selective Homonuclear Polarization Transfer Spectroscopy. *J Magn Reson* **170,** 290-298 (2004).

26. M. Marjanska, P-G. Henry, P.J. Bolan, B. Vaughan, E.R. Seaquist, R. Gruetter, K. Ugurbil, M. Garwood. Uncovering Hidden In Vivo Resonances Using Editing Based on Localized TOCSY. *Magn Reson Med* **53**, 783-789 (2005).

27. M.A. Thomas, N. Hattori, M. Umeda, T. Sawada, S. Naruse. Evaluation of Two-Dimensional L-COSY and JPRESS Using a 3T MRI scanner: From Phantoms to Human Brain *In Vivo*. *NMR Biomed* **16**, 245-251 (2003).

28. J.E. Jensen, B.deB. Frederick, L. Wang, J. Brown, P.F. Renshaw. Two-Dimensional J-Resolved Spectroscopic Imaging of GABA at 4 Tesla in the Human Brain. *Magn Reson Med* **54,** 783-788 (2005).

29. I. Tkac, Z. Starcuk I-Y. Choi, R. Gruetter. In Vivo ^{1}H NMR Spectroscopy of Rat Brain at 1 ms Echo Time. *Magn Reson Med* **41**, 649-656 (1999).

30. I. Tkac, R. Rao, M.K. Georgieff, R. Gruetter. Developmental and Regional Changes in the Neurochemical Profile of the Rat Brain Determined by In Vivo ^{1}H NMR Spectroscopy. *Magn Reson Med* **50**, 24-32 (2003).

31. J. Pfeuffer, C. Juchem, H. Merkle, A. Nauerth, N.K. Logothetis. High-Field Localized ^{1}H NMR Spectroscopy in the Anesthetized and in the Awake Monkey. *Magn Reson Imag* **22,** 1361-1372 (2004).

32. O. Natt, V. Bezkorovaynyy, T. Michaelis, J. Frahm. Use of Phased Array Coils for a Determination of Metabolite Concentrations. *Magn Reson Med* **53**, 3-8 (2005).

33. J. Theberge, R Menon, P.C. Williamson, D.J. Drost, Implementation Issues of Multivoxel STEAM Localized ^{1}H Spectroscopy. *Magn Reson Med* **53**, 713-718 (2005).

34. K. Zong and T Ernst. Localized In Vivo Human 1H MRS at very Short Echo Times. *Magn Reson Med* **52,** 898-901 (2004)

35. F Schubert, J. Gallinat, F. Seifert, H. Rinneberg. Glutamate Concentrations in Human Brain Using Single Voxel Proton Magnetic Resonance Spectroscopy at 3.0 T. *NeuroImage* 21, 1762-1771 (2004).

36. B.J. Soher, P.M. Pattany, G.B. Matson, A.A. Maudsley, Observation of Coupled 1H Resonances at Long TE. *Magn Reson Med* **53,** 1283-1287 (2005).

37. R. Hurd, N. Sailasuta, R. Srinivasan, D.B. Vigneron, D. Pelletier, S.J. Nelson. Measurement of Brain Glutamate Using TE-Averaged PRESS at 3.0 T. *Magn Reson Med* **51,** 435-440 (2004).

38. R.B. Thompson, P.S. Allen. Sources of Variability in the Response of Coupled Spins to the PRESS Sequence and their Potential Impact on Metabolite Quantification. *Magn Reson Med* **41,** 1162-1169 (1999).

39. R.A. de Graaf, Y. Luo, M. Terpstra, M. Garwood. Spectral Editing with Adiabatic Pulses. *J Magn Reson* **B 109,** 184-193 (1995).

40. M. Garwood, L. DelaBarre. The Return of Frequency Sweep: Designing Adiabatic Pulses for Contemporary NMR. *J Magn Reson* **153,** 155-177 (2001).

41. P. Kinchesh, R.J. Ordidge. Spin-echo MRS in Humans at High Field: LASER localization Using FOCI Pulses. *J Magn Reson* **175,** 30-43 (2005)

42. J. Shen, K.F. Petersen, K.L. Behar, P. Brown, T.W. Nixon, G.F. Mason, O.A.C. Petroff, G.I. Shulman, R.G. Shulman, D.L. Rothman. Determination of the Rate of Glutamate/Glutamine Cycle in the Human Brain by *In Vivo* ^{13}C NMR. *Proc. Natl. Acad. Sci.* **96**, 8235-8240 (1999).

43. S. Li, Z. Chen, Y. Zhang, M. Lizak, J. Bacher, R.B. Innis, J. Shen. *In Vivo* Single-Shot, Proton-Localized ^{13}C MRS of Rhesus Monkey Brain. *NMR Biomed* **18**, 560-569 (2005).

44. M.R. Bendall, D.T. Pegg, D.M. Doddrell, J. Field. NMR of protons coupled to ^{13}C nuclei only. *J Am Chem Soc* **103** 934 –936 (1981)

45. R.A. de Graaf, P.B. Brown, G.F. Mason, D.L. Rothman, K.L. Behar. Detection of [1,6-13C2]-Glucose metabolism in rat brain by in vivo 1H-[13C]-NMR spectroscopy. *Magn Reson Med* **49** 37– 46 (2003).

46. F. Boumezbeur, L. Besret, J. Valette, F. Vaufrey, P-G. Henry, V. Slavov, E. Giacomini, P. Hantraye, G. Bloch, V. Lebon. NMR measurement of brain oxidative metabolism in monkeys using 13C-labelled glucose without a ^{13}C radiofrequency channel. *Magn Reson Med* **52** 33–40 (2004).